Structural and biophysical analyses of the skeletal dihydropyridine receptor β subunit β_{1a} reveal critical roles of domain interactions for stability

Received for publication, October 19, 2016, and in revised form, March 16, 2017 Published, Papers in Press, March 28, 2017, DOI 10.1074/jbc.M116.763896

Nicole C. Norris[‡1], Soumya Joseph[‡1], Shouvik Aditya[‡], Yamuna Karunasekara[‡], Philip G. Board[‡], Angela F. Dulhunty[‡], Aaron J. Oakley[§], and Marco G. Casarotto[‡2]

From the [‡]John Curtin School of Medical Research, Australian National University, Canberra, Australian Capital Territory 2601, Australia and the §Department of Chemistry, University of Wollongong, Wollongong, New South Wales 2522, Australia

Edited by Norma Allewell

Excitation-contraction (EC) coupling in skeletal muscle requires a physical interaction between the voltage-gated calcium channel dihydropyridine receptor (DHPR) and the ryanodine receptor Ca^{2+} release channel. Although the exact molecular mechanism that initiates skeletal EC coupling is unresolved, it is clear that both the α_1 and β subunits of DHPR are essential for this process. Here, we employed a series of techniques, including size-exclusion chromatography-multi-angle light scattering, differential scanning fluorimetry, and isothermal calorimetry, to characterize various biophysical properties of the skeletal DHPR β subunit β_{1a}. Removal of the intrinsically disordered N and C termini and the hook region of β_{1a} prevented oligomerization, allowing for its structural determination by X-ray crystallography. The structure had a topology similar to that of previously determined β isoforms, which consist of SH3 and guanylate kinase domains. However, transition melting temperatures derived from the differential scanning fluorimetry experiments indicated a significant difference in stability of ~2–3 °C between the β_{1a} and β_{2a} constructs, and the addition of the DHPR α_{1s} I-II loop (α-interaction domain) peptide stabilized both β isoforms by ~6–8 °C. Similar to other β isoforms, β_{1a} bound with nanomolar affinity to the α-interaction domain, but binding affinities were influenced by amino acid substitutions in the adjacent SH3 domain. These results suggest that intramolecular interactions between the SH3 and guanylate kinase domains play a role in the stability of β_{1a} while also providing a conduit for allosteric signaling events.

Dihydropyridine receptors (DHPRs)[3] are multi-subunit voltage-gated calcium channels that play an essential role in a variety of biological processes including muscle contraction, insulin secretion, and synaptic transmission. The DHPR is made up of a major, pore-forming, α_1 subunit with associated α_2, δ, and β subunits and, in skeletal muscle, α and γ subunits (see Fig. 1*a*). Key elements of the DHPR involve the voltage sensor and the Ca^{2+} ion pore, which are located in the α subunit (α_{1s}), whereas other subunits are essential for correct α_{1S} Ca^{2+} signaling, channel gating, and surface expression (1). DHPR α_{1s} is the largest of the DHPR subunits consisting of four transmembrane repeats that are connected by a series of loops. These loops are linked to the cytoplasmic β subunit, which in the case of skeletal muscle interacts with ryanodine receptor and initiates skeletal EC coupling (2). The structure of the skeletal α_1 subunit was initially solved to an overall resolution of 4.2 Å (3) and more recently to 3.6 Å (4) using cryo-electron microscopy. However, the β_{1a} component of these structures was resolved by docking the structure of the β_{2a} isoform (PDB code 4DEY) caused by the unavailability of the β_{1a} structure. It would therefore be useful if the structure of the β_{1a} were to be determined. Similar to other DHPR β subunits, β_{1a} is made up of a core Src-3 (SH3)-guanylate kinase (GK) module, with the SH3 domain split by a hook region of unknown function (see Fig. 1*b*) (5–7). The SH3 and GK domains are conserved in the β subunits, but the hook and N- and C-terminal regions show greater sequence diversity. It is known that the β subunit is anchored to α_1 through a high affinity (~5–50 nM) interaction (8) through its GK domain via the I-II loop of α_1 (α-interaction domain (AID)). Other lower affinity α_1/β interactions confer isoform-specific functions on α_1 (8).

A number of studies have investigated the isoform-specific properties of the various β subunit domains. A dynamic exchange study of β subunits *in situ* revealed that the β_{1a} formed a stable complex, whereas the other isoforms interacted in a dynamic fashion with their α_1 subunits (9). It is also understood that a unique element of β_{1a} lies in its C-terminal domain where a subset of residues is critical in the communication between the DHPR and ryanodine receptor (10). The importance of the β_{1a} C-terminal domain has been subsequently confirmed in a number of studies in both mouse (11) and zebrafish

The work was supported by grants from Australian National Health and Medical Research Council Grants APP1020589 and APP1002589 (to A. F. D., P. G. B., A. J. O., and M. G. C.) The authors declare that they have no conflicts of interest with the contents of this article.

The atomic coordinates and structure factors (code 4ZW2) have been deposited in the Protein Data Bank (http://wwpdb.org/).

This article contains supplemental Figs. S1 and S2.

[1] Both authors contributed equally to this work.

[2] To whom correspondence should be addressed: John Curtin School of Medical Research, Australian National University, P.O. Box 334, Canberra, ACT 2601 Australia. Fax: 61-2-6125-0415; E-mail: Marco.Casarotto@anu.edu.au.

[3] The abbreviations used are: DHPR, dihydropyridine receptor; ITC, isothermal calorimetry; AID, α-interaction domain; GK, guanylate kinase; PDB, Protein Data Bank; SH, Src homology; MAGUK, membrane-associated guanylate kinase; SEC-MALS, size-exclusion chromatography-multi-angle light scattering; DSF, differential scanning fluorimetry; IPTG, isopropyl β-D-thiogalactopyranoside; EC, excitation-contraction; RT, arginine and threonine.

© 2017 by The American Society for Biochemistry and Molecular Biology, Inc. Published in the U.S.A.

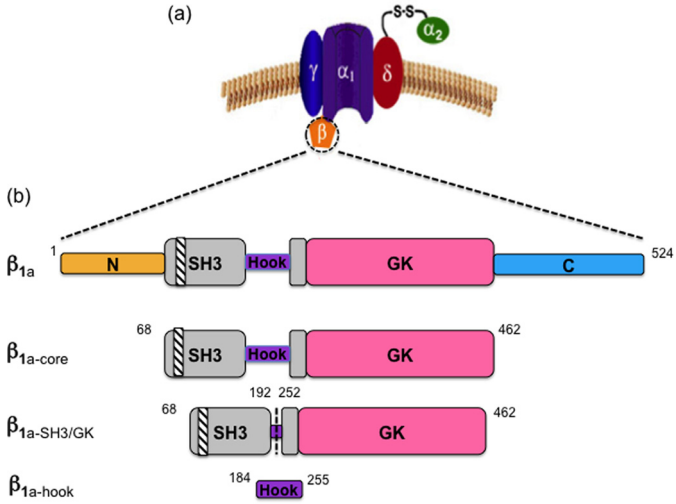

Figure 1. Schematic representation of the DHPR subunits. *a*, diagram outlining the skeletal DHPR subunits. *b*, the domain architecture of β_{1a} illustrating a split SH3 domain (*gray*), which contains a polyproline binding site (*diagonal stripes*). The GK domain is shown in *pink*. The N and C termini (*orange* and *cyan*) and the hook region (*purple*) are intrinsically disordered. Modified β_{1a} constructs ($\beta_{1a\text{-core}}$, $\beta_{1a\text{-SH3/GK}}$, and $\beta_{1a\text{-hook}}$) are illustrated.

myotubes (12); the latter study also identified the β_{1a} SH3 domain as a distinctive determinant for voltage sensing in skeletal muscle. From these works, there is a growing body of evidence that the β_{1a} isoform could possess diverse functional traits compared with the other three isoforms (β_{2a}, β_3, and β_4), and the structural make-up of β_{1a} may be a determining factor driving these novel functions.

Structural determination of full-length β subunits has not been not possible for two main reasons. First, β subunits have a tendency to aggregate at high concentrations (13), and second, the disordered C- and N-terminal domains and the hook region most likely impact upon their ability to crystallize. Therefore to overcome both of these obstacles and aid in the crystallization of β subunit proteins, it has been necessary to remove the disordered regions including the N- and C-terminal domains and in some cases the hook region. The core structures of three different β subunit isoforms (β_{2a}, β_3, and β_4) have been solved (some with AID) with all three isoforms displaying very similar structures that resemble a family of membrane-associated guanylate kinase (MAGUK) proteins (5–7, 14).

In this study we have determined the structure of the DHPR β_{1a} core by X-ray crystallography. We also demonstrate key differences in the biophysical properties of β_{1a} compared with the β_{2a} isoforms by examining their stability and affinity with AID. Although there is high sequence homology between these two isoforms, subtle amino acid differences may be responsible for many of these biophysical differences. The capacity of the SH3 domain and the GK domains to interact with each other is an inherent feature of all β subunits, and the degree and mode of this interaction may play a role in conferring binding to various partner molecules.

Results

Oligomeric state of β_{1a} subunit constructs

The β subunit protein constructs used in this study are shown in Fig. 1*b* and were purified to homogeneity as described under "Experimental procedures." All tags were cleaved prior to experiments being performed, and the minor variation in pH for the different experiment types did not in any way impact upon the conclusions reached.

As part of the initial characterization of protein constructs, the solution molecular masses of β_{1a} constructs were determined using size-exclusion chromatography-multi-angle light scattering (SEC-MALS) and are summarized in Table 1. This included the full-length protein (β_{1a}), a core construct in which the unstructured termini are absent ($\beta_{1a\text{-core}}$), and a construct that consisted only of structured folded domains (SH3 and GK) linked by a residual hook ($\beta_{1a\text{-SH3/GK}}$). β_{1a} eluted as two peaks; the first as a large (megadalton), soluble aggregate eluting at 8 ml, whereas the smaller peak was consistent with the monomer size of ~58 kDa (Fig. 2*a*). The $\beta_{1a\text{-core}}$ construct eluted as multiple peaks, with a range of molecular masses including a large soluble aggregate (Fig. 2*b*). The non-integer values observed for each oligomeric state may be indicative of a protein in slow exchange between multiple states in solution and could explain why, despite multiple attempts, the $\beta_{1a\text{-core}}$ did not crystallize. The smaller $\beta_{1a\text{-SH3/GK}}$ construct eluted as a single, predominantly monodispersed peak with an experimental mass close to its predicted value peak of ~37 kDa (Fig. 2*c*). To determine whether the excised hook region was responsible for the oligomerization of β_{1a}, the hook region ($\beta_{1a\text{-hook}}$) was expressed and examined by several techniques including SEC-MALS, circular dichroism, and NMR. The SEC-MALS profile (Fig. 2*d*) shows that the isolated hook region is monomeric, whereas the CD profile and NMR spectral dispersion indicate that the hook is disordered in solution (supplemental Fig. S1). To examine whether the hook region could induce oligomerization by interacting with $\beta_{1a\text{-SH3/GK}}$, a titration experiment involving these two fragments was performed. Given that no labeled $\beta_{1a\text{-hook}}$ peaks shifted upon addition of $\beta_{1a\text{-SH3/GK}}$ (data not shown), it is reasonable to conclude that here is no evidence of any self-interaction between these two components in full-length β_{1a}.

Structure of the β_{1a} subunit ($\beta_{1a\text{-SH3/GK}}$)

Because of the monomeric nature of $\beta_{1a\text{-SH3/GK}}$, this construct was selected for crystallographic analysis. Despite trialling numerous crystal screening conditions, $\beta_{1a\text{-SH3/GK}}$ could only be crystallized in the presence of the I-II loop (AID) peptide: a clear point of distinction from the β_{2a} and β_3 isoforms where structures have been solved with and without AID. We solved the structure of $\beta_{1a\text{-SH3/GK}}$ to a resolution of 1.83 Å by PHASER (15), using the structure of the rat β_{2a} homolog in complex with an α subunit peptide (PDB code 1T0J). The $\beta_{1a\text{-SH3/GK}}$ structure bears a marked similarity with the structures of other isoforms (Fig. 3*a*) (5–7) displaying backbone root mean square deviations of 0.64, 0.74, and 0.89 Å with β isoforms 2a (PDB code 1T0H), 3 (PDB code 1VYT), and 4 (PDB code 1VYU) (over 265, 269, and 268 C-α atoms, respectively). Briefly, the structure is made up of well-conserved SH3 and GK domains sharing some of the features observed for the MAGUK family of proteins (Fig. 3*a*). The SH3 domain consists of five antiparallel β-strands with the truncated hook region separating the fourth and fifth β-strands. The SH3 domain and its RT-loop are sandwiched between an N-terminal helix (α_1) and

Table 1

The oligomeric state of β_{1a} constructs

The oligomeric state of β_{1a} constructs in solution was calculated by dividing the observed weight-averaged molecular mass with that of the theoretical monomer. Molecular masses greater than 1 MDa eluted close to the void volume of the gel-filtration column and furthermore cannot be accurately determined by MALS; thus they have been designated as "aggregated" protein. Errors in the calculation of observed molecular mass are given. The average protein concentration (μM) corresponding to each peak at the detector is given.

Protein	Molecular mass (kDa)		Oligomeric state	[Protein] @ refractometer μM
	Observed	Theoretical monomer		
β_{1a}	>1000		Aggregate	
	57.1 ± 1.1	57	1.00	0.27
$\beta_{1a\text{-core}}$	>1000		Aggregate	
	104 ± 1		2.42	0.35
	67 ± 0.8		1.56	0.89
	38 ± 0.1	43	0.88	0.86
	29 ± 0.1		Contaminant	
$\beta_{1a\text{-SH3/GK}}$	35.2 ± 0.2	37.2	0.95	9.7
$\beta_{1a\text{-hook}}$	11.0	9.6	1.14	
BSA[a]	200 ± 1.6		2.99	0.38
	132.8 ± 0.5		1.98	1.2
	67.1 ± 0.1	67	1.00	6.8

[a] BSA was not monomeric.

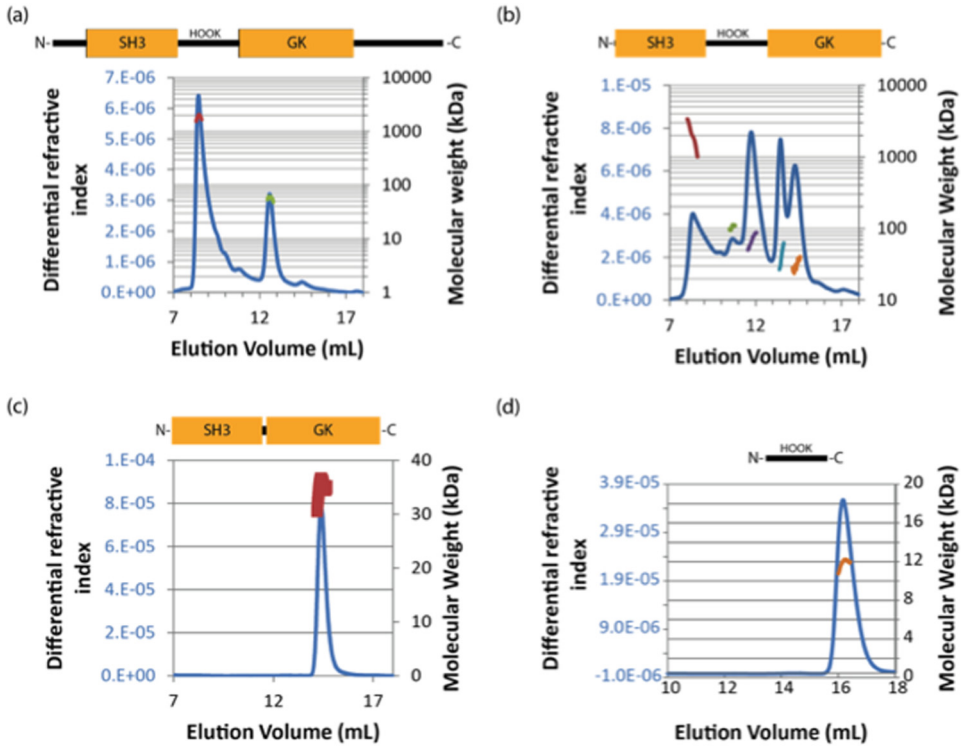

Figure 2. The solution molecular mass(es) of β_{1a} constructs. Full-length β_{1a} (*a*), $\beta_{1a\text{-core}}$ (*b*), $\beta_{1a\text{-SH3/GK}}$ (*c*), and $\beta_{1a\text{-hook}}$ (*d*) constructs were analyzed by SEC-MALS. Proteins (0.1 mg) were applied to an analytical Superdex 200 size exclusion column. They were eluted in 20 mM Tris-HCl at pH 8.0 and 150 mM potassium chloride at room temperature. Samples were reduced with 1 mM dithiothreitol prior to application. The elution profile was monitored by the change in refractive index (*continuous blue line*). The molecular masses (kDa; *secondary axis*) corresponding to peaks are shown as discrete points. Bovine serum albumin (non-monomeric) was analyzed as a standard.

another helix that lies C-terminal to β4 (α_2) through a network of hydrophobic interactions. The structure of all isoforms thus far examined show that the canonical SH3 polyproline-binding site is occluded by the RT-loop and the α_2 helix, and this is also true for β_{1a} (Fig. 3*a*). The GK domain consists of a five-stranded parallel β-sheet surrounded by six α-helices and forms an intramolecular interaction with the SH3 domain through a series of hydrogen bond and van der Waals contacts. The I-II loop AID peptide binds the GK domain in a hydrophobic groove that is situated on the opposite side of the SH3 domain. Similar to the other β isoforms, upon binding the DHPR I-II loop (AID) adopts an α-helical conformation that predominantly contacts the α_3, α_6, and α_9 helices of β_{1a} by means of several hydrophobic contacts and to a lesser extent hydrogen bond and ionic interactions as displayed in Fig. 3*b*.

Thermal stability of $\beta_{1a\text{-SH3/GK}}$ versus $\beta_{2a\text{-SH3/GK}}$ constructs

The thermal stability of a protein is often a good indicator of its crystallization potential and is typically used to screen for crystallization conditions (16). Because it was possible to crystallize $\beta_{2a\text{-SH3/GK}}$ but not $\beta_{1a\text{-SH3/GK}}$ in the absence of AID, the temperature stability of both core constructs were examined using DSF. For all constructs (Fig. 4*a*), the transition melting curves showed only one inflection point (Fig. 4*b*), suggesting

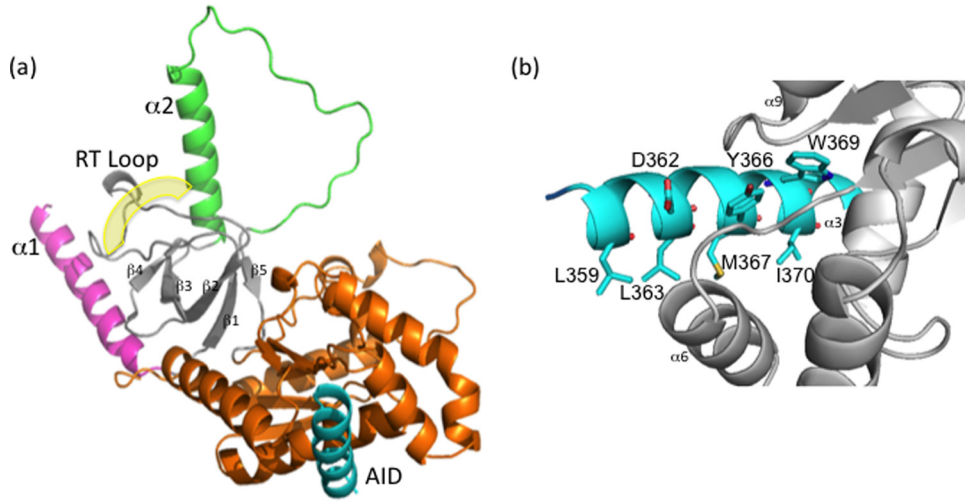

Figure 3. X-ray crystal structure of DHPR $\beta_{1a\text{-}SH3/GK}$ complexed with AID peptide. *a*, cartoon representation of the DHPR $\beta_{1a\text{-}SH3/GK}$ complexed with AID. The split architecture of the SH3 domain is shown in *gray* with its labeled RT-loop highlighted. The RT-loop is sandwiched between the α_1 (*pink*) and α_2 helices (*green*), which are involved in the occlusion of the polyproline binding site. The GK domain is displayed in *orange*, and the DHPR I-II AID peptide binding ligand is in *blue*. The *yellow shading* denotes the putative polyproline binding site. *b*, close-up of the interaction between the AID peptide (*blue*) and $\beta_{1a\text{-}SH3/GK}$ (*gray*) highlighting contributing residues facilitating AID binding.

that either the SH3 and GK domains unfolded independently at similar temperatures or, more likely, because of their ability to interact, a synergic unfolding event had taken place. The T_m values of all $\beta_{SH3/GK}$ constructs are summarized in Fig. 4*c*. $\beta_{1a\text{-}SH3/GK}$ was found to be ~3 °C less stable than $\beta_{2a\text{-}SH3/GK}$, whereas the addition of AID increased the T_m of $\beta_{2a\text{-}SH3/GK}$ by ~6.5 °C and $\beta_{1a\text{-}SH3/GK}$ by ~8 °C, respectively, indicating the extent that AID stabilizes these constructs. These results may explain the difficulties surrounding the crystallization $\beta_{1a\text{-}SH3/GK}$ and why the addition of AID facilitates this process. As part of our preliminary studies, DSF studies were also performed with the full hook region ($\beta_{1a\text{-}core}$). This experiment revealed a ~3° reduction in T_m compared with truncated core ($\beta_{1a\text{-}SH3/GK}$). The addition of AID did stabilize $\beta_{1a\text{-}core}$ to similar level as seen for $\beta_{1a\text{-}SH3/GK}$, but neither the stand-alone protein nor its AID complex could be crystallized despite using a variety of screening conditions.

To determine which regions of the β subunits are responsible for their differences in stability, we have analyzed the sequences of all four β isoforms. Fig. 5*a* shows that the β_{1a} isoform most resembles β_{2a}, with a sequence identity of 60%. This value increased to 78% upon removal of the N- and C-terminal domains and hook region (Fig. 5*b*). Further deletion of the GK domain only resulted in a modest 2% increase in homology (Fig. 5*c*), whereas a 13% increase was observed by deletion of the SH3 domain (Fig. 5*d*), indicating that the SH3 domain is primarily responsible for the sequence diversity between core region of β_{1a} and β_{2a}. Based on this analysis, it is evident that the SH3 domain displays a level of sequence diversity among the β isoforms that warrants further investigation; therefore two β-chimeras were constructed and subjected to thermal denaturation. Substitution of the β_{1a} SH3 domain onto a β_{2a} background ($\beta_{1a\text{-}SH3/\beta2aGK}$) resulted in a reduced T_m compared with the $\beta_{2a\text{-}SH3/GK}$ (Fig. 4, *b* and *c*). A reduction in T_m was also evident upon substitution of the β_{1a} SH3 RT-loop onto a β_{2a} background ($\beta_{2a\text{-}SH3(\beta1aRT)/GK}$), indicating that unique sequence elements in the SH3 domain of β_{1a} increase the temperature instability for the $\beta_{1a\text{-}SH3/GK}$. This suggests that from a thermal stability viewpoint, the SH3 domain of the two isoforms β_{1a} and β_{2a} are not interchangeable.

Affinity measurements of $\beta_{SH3/GK}$ constructs and the DHPR AID peptide

Previous binding values between β subunits and AID peptides have been measured to range between 5 and 50 nM (8); however, the affinity between β_{1a} and its corresponding AID peptide has not been measured. The affinities of various $\beta_{SH3/GK}$ constructs for the DHPR AID peptide were measured using isothermal calorimetry (ITC) and showed stoichiometric binding of 1:1 (Fig. 6 and Table 2). The affinity of $\beta_{1a\text{-}SH3/GK}$ for skeletal AID was measured to be 4.9 ± 2.1 nM, whereas a value of 17.1 ± 3.3 nM was observed for $\beta_{2a\text{-}SH3/GK}$. Substitution of the β_{1a} RT-loop onto β_{2a} ($\beta_{2a\text{-}SH3(\beta1aRT)/GK}$) had a negligible effect on binding (16.5 ± 4.2 nM), but replacing the entire SH3 domain ($\beta_{1a\text{-}SH3/\beta2aGK}$) increased the affinity (7.0 ± 2.8 nM) to values comparable with that observed for β_{1a}.

Discussion

In contrast to other DHPR β subunit isoforms, β_{1a} is expressed only in skeletal muscle and is an exclusive partner of DHPR α_{1s}. β_{1a} is also essential in the functional assembly of skeletal muscle triads and is required to form DHPR tetrads (17). Given the unique functional features of β_{1a}, it has been important to characterize its structural and biophysical properties. Isolated, full-length β_{1a} exists primarily in large, multimeric assemblies. Removal of the instrinsically disordered N- and C-terminal regions shifted its oligomerization profile, resulting in a series of multi-sized aggregates, whereas further excision of the hook region gave rise to a well-behaved monomeric species. This indicates that the hook region is intimately involved in the oligomerization process. CD, SEC-MALS, and NMR confirmed that the hook region is monomeric and intrinsically disordered but, based on NMR titration experiments, is unlikely to promote oligomerization by interacting with the β_{1a}

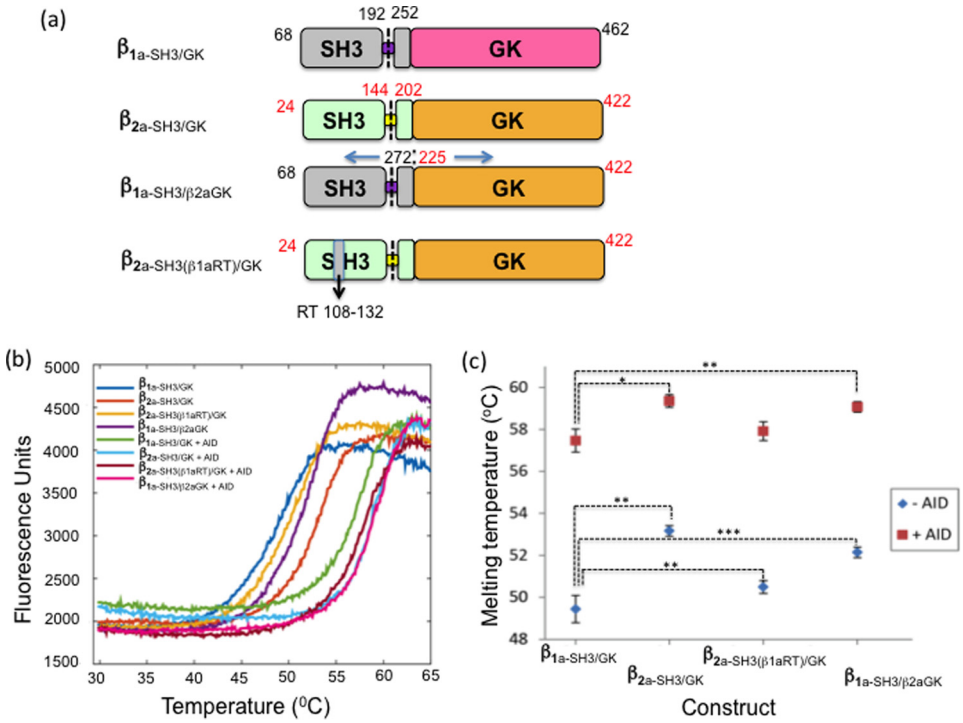

Figure 4. Thermal denaturation measurements of $\beta_{SH3/GK}$ constructs in the absence and presence of AID peptide. *a*, amino acid composition of $\beta_{SH3/GK}$ constructs (*black* and *red numbers* denote β_{1a} and β_{2a}, respectively). *b*, temperature denaturation curves for selected $\beta_{SH3/GK}$ constructs with and without AID. *c*, summary of transition melting temperatures for the constructs $\beta_{1a\text{-SH3/GK}}$, $\beta_{2a\text{-SH3/GK}}$, $\beta_{2a\text{-SH3}(\beta1aRT)GK}$, and $\beta_{1aSH3/\beta2aGK}$. Each data set represents two independent sets of quadruplicate measurements. Paired Student's *t* test analyses for ± AID were performed relative to $\beta_{1a\text{-SH3/GK}}$. *, $p < 0.05$; **, $p < 0.01$; ***, $p < 0.001$.

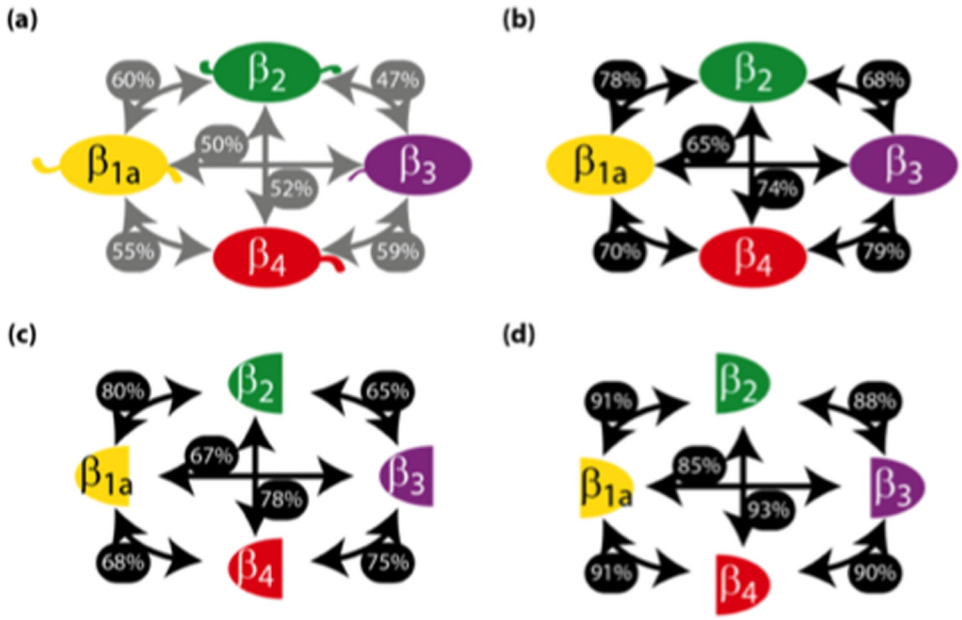

Figure 5. DHPR-β isoforms have high sequence identity and structural similarity. The primary sequences of the mouse protein cores, which matched the primary sequence of solved crystal structures (β_{1a}, A2A4545$_{58-454}$; β_2, Q8CC26$_{68-485}$; β_3, P54285$_{16-375}$; and β_4, Q8R0S4$_{48-398}$), were aligned pairwise using ClustalO. The boundaries of the core were defined by Simple Molecular Architecture Research Tool (SMART) and encompassed the VGCC domain through to the guanylate kinase domain. *a*, β; *b*, $\beta_{SH3/GK}$; *c*, β SH3 domain; *d*, β GK domain. The sequence identity is shown as a percentage beside the *arrows* linking each isoform.

core SH3 and GK domains. Although the exact role of the hook region in oligomerization of β_{1a} remains undefined, a possible role may be to enable domain swapping between the SH3 and GK domains, a hypothesis first proposed for another MAGUK protein, PSD-95 (18). The functional role of the hook region from various β isoforms has been examined previously and identified as an important element in regulating DHPR channel inactivation (19). In the case of β_{1a}, removal of the hook region has been reported to reduce intracellular calcium release (12). What is unknown and of future interest is whether the hook

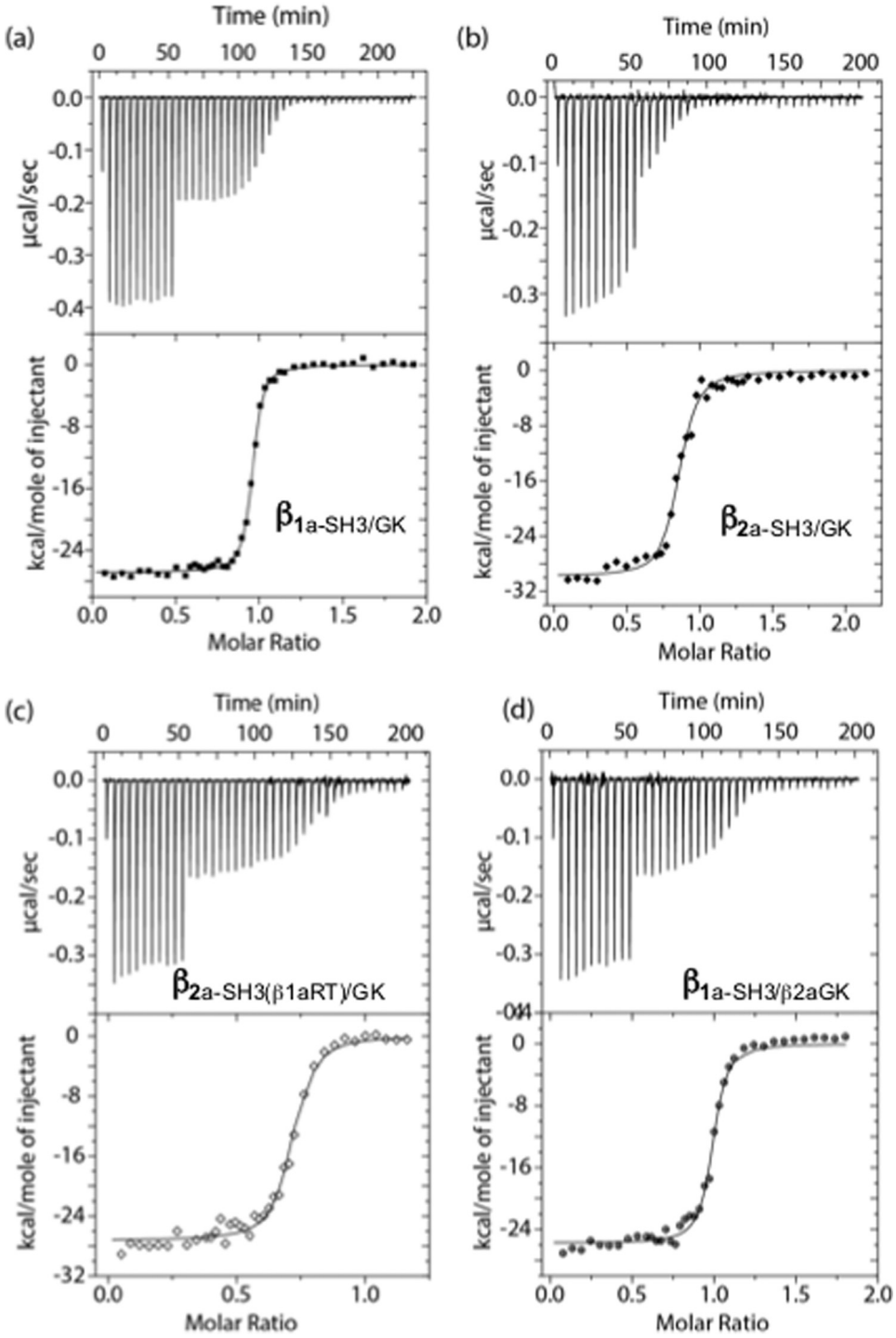

Figure 6. ITC curves for $\beta_{SH3/GK}$ constructs titrated with AID. ITC isotherms and curves for the constructs $\beta_{1a\text{-}SH3/GK}$ (*a*), $\beta_{2a\text{-}SH3/GK}$ (*b*), $\beta_{2a\text{-}SH3(\beta1aRT)GK}$ (*c*), and $\beta_{1aSH3/\beta2aGK}$ (*d*). Binding and thermodynamic parameters are displayed in Table 2.

Table 2
Collated ITC data for $\beta_{\text{-}SH3/GK}$ constructs titrated with AID

	n	K_D	*t* test *p* value (to $\beta_{1a\text{-}SH3/GK}$)	*N*	Δ*H*	Δ*S*	Δ*G*
		nM			*kCal/mol*	*Cal/mol·K*	*kJ/mol*
$\beta_{1a\text{-}SH3/GK}$	3	4.9 ± 2.1	NA[a]	0.96	−27.1	−52.6	−45.7
$\beta_{2a\text{-}SH3/GK}$	3	17.1 ± 3.3	0.013	0.80	−29.33	−62.7	−42.6
$\beta_{2a\text{-}SH3(\beta1aRT)/GK}$	3	16.5 ± 4.2	0.002	0.72	−26.8	−54.2	−44.8
$\beta_{1a\text{-}SH3/\beta2aGK}$	3	7.0 ± 2.8	0.26	1.01	−23.6	−41.8	−46.5

[a] NA, not applicable.

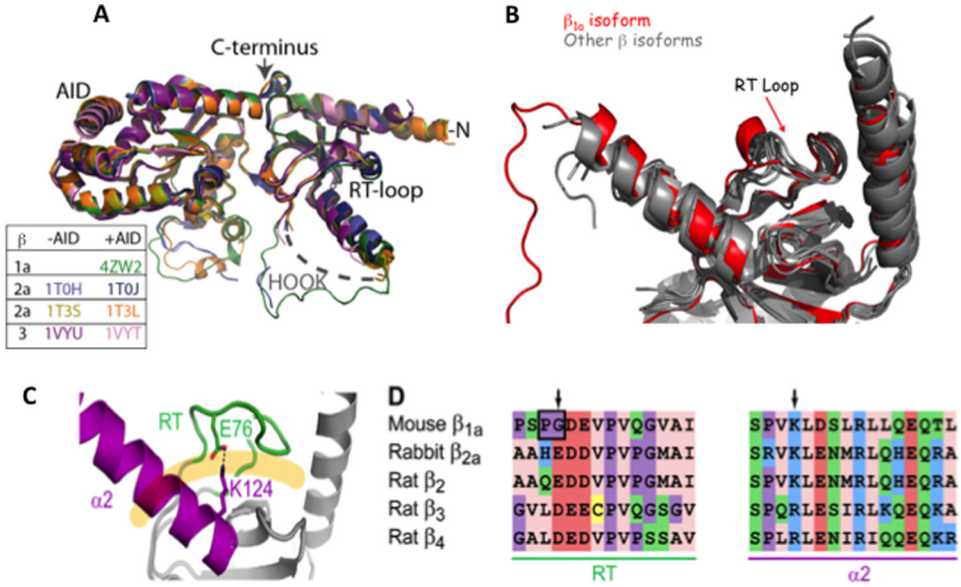

Figure 7. Structural comparisons between β_{1a} isoforms. *A*, backbone superposition of β_{1a} with structures that have been crystallized with and without AID peptide. The color key corresponds to β isoforms. *B*, overlay of β X-ray crystal structures showing the SH3 domain, the α_1 and α_2 helices, and the RT-loop. The β_{1a} structure is depicted in *red*. *C*, the X-ray crystal structure of the SH3 domain of rabbit β_{2a} (PDB code 1t3l). The α_2 helix and the RT-loop are highlighted in *magenta* and *green*, respectively, and interact through a salt bridge involving the side chains of Glu^{76} and Lys^{124} (shown). These structural elements occlude the polyproline binding site, which is displayed as a *pale orange line*. The sequence alignment of the α_2 helix and the RT-loop is displayed for all β-subunit isoforms with the *arrows* denoting charged residues involved in a salt bridge that is absent in the β_{1a} RT-loop.

region that plays a role in the aggregation of β_{1a} *in vitro* is implicated in DHPR tetrad formation?

The crystal structure of the monomeric $\beta_{1a\text{-SH3/GK}}$ complexed with the AID peptide has been solved to a resolution of 1.86 Å, making it the most highly resolved β-structure so far determined. As shown in Fig. 7*A*, the structure shows a high degree overlap with structural elements from other β-structures with the only real point of difference visible in loop regions in GK domain between strand β7 and helix α5, as well as the residual hook region. Although the majority of hook region has been removed, the remaining hook residues display a well-defined loop structure. As previously discussed, the β_{1a} SH3 domain exhibits the greatest sequence variation between the β isoforms; therefore it was of interest to focus more closely on this region. Despite a clear difference in the composition of the β_{1a} SH3 RT-loop between various isoforms, this region reveals a remarkable degree of overlap with other β-structures (Fig. 7*B*) with the RT-loop stabilized by a series of hydrophobic interactions between the two α-helical segments effectively occluding the canonical SH3 binding site. A clear point of difference in this structure, however, is the absence of a salt bridge between an acidic RT-loop and a conserved basic residue in α_2, which is present in other β isoform structures (Fig. 7*C*). It is likely that this interaction may help in stabilizing the position of the RT-loop.

This argument is strengthened by the T_m measurements performed for the various β constructs. Comparison of core $\beta_{1a\text{-SH3/GK}}$ and $\beta_{2a\text{-SH3/GK}}$ consistently showed a marked difference in their T_m values of ~3° with $\beta_{2a\text{-SH3/GK}}$ showing greater stability. Substitution of the β_{1a} SH3 domain or the SH3 β_{1a} RT-loop onto a β_{2a} background served to lower the T_m values with respect to β_{2a}, suggesting that the presence of specific amino acid residues within the β_{2a} SH3 domain (in particular the RT-loop) stabilized the protein. The addition of the AID peptide resulted in a striking T_m increase for all constructs ranging from a maximum ~8° C increase in $\beta_{1a\text{-SH3/GK}}$ to a minimum of ~6.5° C in $\beta_{2a\text{-SH3/GK}}$. This increase in T_m suggests that β_{1a} exhibits a less stable, more dynamic structure that is markedly stabilized by the addition of AID, thereby facilitating crystallization. Even though there is an increase in the stability of $\beta_{2a\text{-SH3/GK}}$ upon the addition of AID, its presence is not a prerequisite for the crystallization of β_{2a} (6).

The ITC results performed in this study indicate that the binding affinity of the AID peptide to $\beta_{1a\text{-SH3/GK}}$ is approximately three times tighter than that of $\beta_{2a\text{-SH3/GK}}$, a result that is consistent with the trend observed in the thermal stability experiments (see above). However, of particular note was the K_d obtained for the $\beta_{1a\text{-SH3/}\beta 2a\text{GK}}$ chimera, which was similar to that observed for $\beta_{1a\text{-SH3/GK}}$. This result suggests that despite the AID-binding site being located on the GK domain, changes in the SH3 domain influenced binding on the other side of the molecule. Such an observation can be rationalized by considering the intramolecular interaction between the two domains as seen in all β X-ray crystal structures. In the case where the X-ray structures have been solved for both the apo/β and AID/β complexes (β_2 and β_3 isoforms), there are subtle but clear differences at the GK/SH3 domain interface as observed by changes in salt-bridge and hydrogen-bond connectivities (supplemental Fig. S2) and by overall changes in the buried surface area between the two domains (6). Prior to the structural determination of the AID-binding site, it was assumed that AID interacted with what was described as the β-interaction domain, which spans the SH_3, hook, and GK domains. This assumption was based directly on studies where several β-interaction-domain point mutations directly impacted AID binding (20), a finding that highlights the intricate interaction net-

work that exists throughout the molecule extending from the AID-binding site in the GK domain though to the SH_3 domain. In this context, it is understandable that swapping the SH_3 domain would influence AID binding to the GK domain as observed for the $\beta_{1a\text{-}SH3/\beta2aGK}$ chimera.

The intramolecular interaction between the SH_3 and GK domains may provide a framework that enables allosteric changes to propagate throughout the molecule. A conformational change in β could conceivably be triggered by any number of biological events including depolarization of the surface plasma membrane. Several studies have suggested that the interaction between the β subunit and AID are reversible (9, 21). Interestingly, based on a 3.6 Å cryo-electron microscopy model of DHPR ($Ca_V1.1$), it was predicted that conformational changes in the DHPR α_1 S6 transmembrane helix can be translated through to the β_{1a} subunit via AID, giving rise to the displacement of β_{1a} (4). Based on the findings derived from our study, it is clear that the biophysical properties of β subunits are highly sensitive to AID binding and may be a determining factor that controls its conformation and binding of other partner molecules. Furthermore, the temperature stability and AID-binding profiles observed for $\beta_{1a\text{-}SH3/GK}$ and $\beta_{2a\text{-}SH3/GK}$ are sufficiently different to suggest that the sequence variability between the two isoforms represents another layer of complexity that may give rise to isoform-specific binding partners.

In the past, the role of the β subunit has been limited to enhancing localization of the α subunit to the plasma membrane, as well as regulating calcium channel gating; however, we are now discovering newly assigned functions independent of these roles, including gene regulation (22). A number of studies have openly raised the possibility that the SH3 domain of DHPR β subunits may engage with partner proteins possessing a SH3 recognition motif (P*XX*P) (12, 23); however, the crystal structure of all β subunits show that the traditional SH3 binding site is occluded. The information derived from the present study indicates that the SH3 domain in β_{1a} exhibits a degree of structural plasticity that under certain conditions may allow other proteins possessing SH3 recognition motifs to engage the β_{1a} subunit.

Experimental procedures

Production of recombinant proteins and peptide synthesis

All proteins were expressed recombinantly in *Escherichia coli* (BL21 DE3) in 2× YT supplemented with yeast nitrogen base without amino acids, iron chloride, and the appropriate antibiotic. The DHPR α_{1s} AID peptide (^{357}QQLEEDLRGYMSWITQGE^{374}) was synthesized by the Biomolecular Resource Facility of the John Curtin School of Medical Research (Australian National University, Canberra, Australia) using an Applied Biosystems 430A peptide synthesizer and purified by reverse-phase HPLC on a Jupiter 300 C4 column. Peptides were eluted using a linear gradient from buffer A (deionized water and 0.1% TFA) and buffer B (acetonitrile and 0.1% TFA). Purified peptide fractions were identified by mass spectroscopy using an AB MDS Sciex 4800 MALDI-TOF-TOF mass analyzer.

DHPR β_{1a}

The gene sequence encoding full-length mouse β_{1a} subunit (NCBI code NM_031173) was amplified by PCR. The PCR product was cloned into pHUE (24), which encodes an N-terminal polyhistidine-ubiquitin tag. Transformed bacteria were cultured at 37 °C until $A_{600\,nm}$ = ~0.6. Protein expression was induced by adding isopropyl β-D-thiogalactopyranoside (IPTG) to a final concentration of 0.1 mM. The cells were cultured for a further 3 h. The protein was purified by nickel-agarose chromatography. Ubiquitin was removed by digestion with UBP41 (produced in-house), a polyhistidine-tagged ubiquitin-dependent protease (24). The protein was further purified by preparative electrophoresis using a Bio-Rad model 491 prep cell. The protein was refolded by dialysis into 50 mM sodium phosphate buffered at pH 8 and 300 mM sodium chloride. The protein was concentrated and stored at −80 °C.

DHPR $\beta_{1a\text{-}core}$

The $\beta_{1a\cdot core}$ construct was also expressed with a hexahistidine-ubiquitin tag. Bacteria transformed with pHUE-$\beta_{1a\cdot core}$ were cultured at 37 °C to an $A_{600\,nm}$ level of ~0.6. Protein expression was induced with 0.1 mM IPTG and cultured for 3 h. The bacteria were resuspended in 20 mM Tris-HCl buffered at pH 8.0, 500 mM sodium chloride, and 30 mM imidazole (Buffer O) containing 10% glycerol and EDTA-free protease inhibitor mixture (Roche). The cells were lysed by the addition of lysozyme (1 μg·ml), DNase I (1 μg·ml), and RNase H (1 μg·ml). The suspension was also passed through a French press (3 × 1500 p.s.i.). The cleared lysate was applied to HisTrap column and washed with buffer O and then buffer O containing 1.5 M sodium chloride. The protein was eluted using a gradient of up to 500 mM imidazole in buffer O. The protein was de-ubiquitinylated using UBP41 and simultaneously dialyzed into buffer O containing 5 mM 2-mercaptoethanol. The tag, uncleaved protein, and de-ubiquitinylase were removed by passing the protein solution over HisTrap column. The flowthrough was dialyzed into 20 mM Tris-HCl buffered at pH 8.0 and 50 mM sodium chloride (buffer Q) for 2 h at 4 °C. The protein solution was applied to anion-exchange resin and eluted with buffer Q with a gradient of up to 1 M sodium chloride. The eluate was applied to a size-exclusion column. Peaks containing $\beta_{1a\cdot core}$ were pooled, concentrated to 1 mg·ml^{-1}, snap frozen, and stored at −80 °C.

DHPR $\beta_{SH3/GK}$ constructs ($\beta_{1a\text{-}SH3/GK}$, $\beta_{2a\text{-}SH3/GK}$, $\beta_{1a\text{-}SH3/\beta2aGK}$, and $\beta_{2a\text{-}SH3(\beta1aRT)/GK}$)

Genes encoding hexahistidine-tagged β constructs were synthesized and cloned into a custom vector pJ411^{KanR} with a high copy number origin of replication (DNA 2.0). Truncated and chimeric protein constructs were constructed to include the following residues: $\beta_{SH3/GK}$ (**68–192** ~ **252–462**), $\beta_{2a\text{-}SH3/GK}$ (24–144 ~ 202–422), $\beta_{1a\text{-}SH3/\beta2aGK}$ (**68–192** ~ **252–272** ~ 225–422), and $\beta_{2a\text{-}SH3(\beta1aRT)/GK}$ (24–66 ~ **108–132** ~ 90–144 ~ 202–422), where bold denotes β_{1a} and non-bold denotes β_{2a} numbering. Bacteria transformed with the plasmids were cultured at 37 °C in 2× YT and kanamycin (50 μg·ml^{-1}) to an $A_{600\,nm}$ level of ~0.3. They were further cultured at 16 °C for 1 h. Protein expression was induced with

IPTG (0.4 mM), and the cells were cultured overnight. The bacterial pellet was resuspended in 50 mM phosphate buffer at pH 7.0, 500 mM sodium chloride, and 30 mM imidazole (buffer A) containing an EDTA-free protease inhibitor mixture (Roche), lysozyme (1 $\mu g \cdot ml^{-1}$), DNase I (1 $\mu g \cdot ml^{-1}$), and RNase H ($\mu g \cdot ml^{-1}$). The cells were lysed using a French press (3 × 1500 p.s.i.). The cleared lysate was applied to a HisTrap column. The resin was washed with buffer A and then buffer A containing 1.5 M sodium chloride. The protein was eluted using a gradient of imidazole up to 500 mM. The hexahistidine tag was cleaved with HRV 3C protease (produced in-house) and simultaneously dialyzed overnight in buffer A containing 5 mM 2-mercaptoethanol at 4 °C. The protein solution was applied to nickel-nitrilotriacetic acid resin to remove the hexahistidine tag-containing entities. The flowthrough was further purified by size-exclusion chromatography.

$\beta_{1a\text{-}hook}$

The DNA sequence encoding hexahistidine-tagged HOOK was synthesized and cloned into a custom vector pJ411^{KanR} with a high copy number origin of replication (DNA 2.0). Bacteria transformed with pHis3C^{kanR}-HOOK were cultured at 37 °C in 2× YT and kanamycin (50 $\mu g \cdot ml^{-1}$). Protein expression was induced at an $A_{600\,nm}$ level of ~0.8 by the addition of IPTG (1 mM) and cultured for a further 4 h. The bacteria were resuspended in 20 mM Tris-HCl buffered at pH 8.0, 500 mM NaCl, and 30 mM imidazole (buffer H) containing 6 M guanidine-HCl. The cells were lysed using the French press (3 × 1500 p.s.i.). The cleared lysate was applied to nickel-nitrilotriacetic acid resin and incubated for 30 min at 4 °C. The resin was washed with buffer H containing 6 M urea and then with buffer H. The peptide was eluted with buffer H containing 300 mM imidazole. The acidified (pH < 5.0) eluate was applied to preparative C18 reversed-phase HPLC column. The peptide was eluted with a gradient of acetonitrile over a background of 0.1% trifluoroacetic acid in MilliQ water. The appropriate peaks were lyophilized and stored at −70 °C.

MALS of β_{1a} constructs

Protein (0.1 μg), reduced with 1 mM DTT, was applied to a Superdex 200 Increase analytical column attached to an in-line refractometer and light scatterer (Wyatt). The protein was eluted using 20 mM Tris buffer at pH 8.0 and 150 mM potassium chloride at a flow rate of 0.5 $ml \cdot min^{-1}$ (Waters instrument).

Crystallization of $\beta_{1a\text{-}SH3/GK}$

Initial crystallization trials were conducted at the Collaborative Crystallization Centre (http://www.csiro.au/c3) using the vapor diffusion method. Crystallization conditions were identified using the JCSG+ and PACT screens (25). Protein solution (150 nl) and screening solution (150 nl) were dispensed into the reservoirs of Innovadyne crystallization plates. The drops imaged by Rigaku Minstrel systems at 8 or 20 °C. Crystals were observed to grow in conditions G7 (20% PEG 3350, 0.1 M Bis-Tris propane, pH 7.5, 0.2 M sodium acetate) were selected for optimization. Optimized crystals for X-ray data collection were grown using the hanging-drop vapor diffusion methods using VDX^{TM} plates (Hampton Research). 2-μl drops containing protein were mixed with equal volumes of precipitant (20% PEG 3350, 0.1 M Bis-Tris propane buffered at pH 8.0 and 0.2 M sodium acetate) on siliconized coverslips (Hampton Research), which were suspended over drops containing precipitant. The trays were equilibrated at 5 °C. Crystals appeared in 5 days and reached maximum size (bipyramids with maximum dimension of ~200 μM) in 10 days. MiTeGen loops were used to manipulate crystals. For X-ray data collection, a crystal was transferred to artificial mother liquor containing 25% PEG 3350 for 2 min prior to transfer to flash cooling to 100 K using an Oxford Cryostream. CuKα X-rays were produced by a Rigaku 007HF rotating anode generator with Varimax optics. X-ray data were collected using a Mar345 desktop beamline. Diffraction data were integrated, merged, and scaled with the HKL2000 package (26). The structure was solved by PHASER (15), using the structure of the rat β_{2a} homolog in complex with an α subunit peptide (PDB code 1T0J). Iterative cycles of model building and refinement were performed in COOT (27) and REFMAC5 (28). The X-ray data and model quality are given in Table 3.

Table 3
X-ray data collection and refinement statistics for $\beta_{1a\text{-}SH3/GK}$

X-ray data	
Space group	$P2_12_12_1$
Unit cell parameters	a = 46.2, b = 69.4, c = 131.1 Å; $\alpha = \beta = \gamma = 90°$
Resolution range (Å)[a]	50–1.86 (1.93–1.86)
Total no. of observations	249,097
No. of unique reflections	36,235
$I/\sigma I$	35.45 (4.95)
R_{merge} (%)[b]	5.3 (36.4)
R_{meas} (%)	5.3 (36.4)
$CC_{½}$ (%)	98.8 (93.2)
Completeness	99.8 (99.1)
Multiplicity	6.9 (5.7)
Refinement statistics	
Resolution range (Å)	22.8–1.86 (1.908–1.860)
No. of reflections (R_{work} set)	32,572 (2447)
No. of reflections (R_{free} set)	1801 (108)
R_{work} (%)[c]	16.87 (22.8)
R_{free} (%)	20.70 (29.6)
No. of atoms	3,010
áBñ of structure (Å^2)	15.49
Root mean square deviation from ideal geometry	
Bond lengths (Å)	0.019
Bond angles (°)	1.897
Chiral centers (Å^3)	0.121
General planes (Å)	0.010

[a] The numbers in parentheses refer to the highest resolution bin.
[b] $R_{merge} = \Sigma_h\Sigma_i|I_i - áIñ|/\Sigma_h\Sigma_i I_i$.
[c] $R_{factor} = \Sigma_h|F_{obs} - F_{calc}|/\Sigma_h|F_{obs}|$, where F_{obs} and F_{calc} are the observed and calculated structure factors, respectively. R_{free} was calculated from 5% of the diffraction data not used in refinement.

SYPRO orange thermal denaturation assays of DHPR $\beta_{SH3/GK}$ constructs

The proteins were either dialyzed overnight or gel-filtered (Superdex 200 Increase) in 20 mM HEPES buffered at pH 7.5, 150 mM sodium chloride, and 1 mM DTT (buffer T). Dialyzed proteins were centrifuged for 10 min at (20,000 × g) to remove aggregated species. The protein (0.1 $mg \cdot ml^{-1}$) solutions were dispensed in a 384-well plate in quadruplicate (EpMotion). SYPRO orange fluorescence (F) was monitored as the plate was heated from 25–90 °C at a rate of 1°/min (Q-PCR 7900). All constructs were analyzed in the presence or absence of 5-fold excess AID. A sigmoid curve (below) with variables corre-

sponding to the gradient (m) and the point of inflection (i) was fitted using either MATLAB or Microsoft Excel. The average of the inflection points was taken as the melting temperature (T_m) for each construct.

$$F = \frac{e^{m(T - i)}}{1 + e^{m(T - i)}} \quad \text{(Eq. 1)}$$

Each T_m represents the mean of two sets of quadruplicate measurements with the error range of the T_m represented by error bars.

ITC of DHPR $\beta_{SH3/GK}$ constructs with AID

DHPR β constructs were exchanged into 10 mM K_3PO_4 buffered at pH 7.0 and 150 mM KCl (buffer C) either using overnight dialysis or size-exclusion chromatography. The AID peptide was dissolved in buffer C, and the pH was adjusted. ITC was conducted in 10 mM potassium phosphate buffered at pH 7.0 and 150 mM potassium chloride at 25 °C using a VP-ITC (MicroCal). The reference power was set to 17 μCal·s^{-1}, and the cell contents were stirred continuously at 300 rpm. We aimed for 50 μM AID in the titration syringe and 5 μM β constructs in the cell, although the true concentration of protein varied slightly between experiments. A small volume (3 μl) was initially injected. The next 10 and final 11 injections were of ~350 pmol to obtain an accurate enthalpy change (ΔH). Smaller injections of ~175 pmol were used to accurately determine gradient of the transition and the point of inflection, which correlate to the affinity (K_A) and stoichiometry (N) of the interaction, respectively. We allowed 5-min delays between injections, which was extended to 6 min when necessary. Heat was corrected for the heat of dilution by titrating AID peptide into buffer using the same titration protocol. A binding isotherm was generated by plotting the heat change for each injection over the total delay interval against the molar ratio of AID to the β construct. The binding isotherm was modeled for a single site using non-linear least squares analysis (Origin 7.0 embedded in MicroCal software). All parameters, which include the stoichiometry (N), binding constant (K_A), and the enthalpy change (ΔH), were allowed to vary during the fitting cycles.

The concentration of titrant (AID) and titrand (β constructs) were determined using a conventional UV-visible range spectrophotometer ($A_{280\,nm} = \epsilon_{cl}$), where $\epsilon_{AID\ @\ 280\ nm} = 6.99$ M^{-1}·cm^{-1}. The corrected extinction coefficients for the β constructs were determined using a conventional UV-visible range spectrophotometer and the theoretical extinction coefficient calculated (29) by ProtParam.

Statistical significance

The K_D values and melting temperatures derived from ITC and DSF experiments, respectively, were analyzed for statistical significance using a paired t test. The criteria for a significant t test is considered to be a p value of <0.05 (30).

Author contributions—N. C. N., S. J., S. A., Y. K., and A. J. O. conducted the experiments, and N. C. N., S. J., A. J. O., P. G. B., A. F. D., and M. G. C. designed the experiments and wrote the paper.

Acknowledgments—We thank Dr. Damien Hall for help fitting curves using MATLAB and Dr. Hideki Onagi for advice on ITC experiments. We also thank the technical staff of the Bio21-C3 Center for help with crystallization.

References

1. Obermair, G. J., Tuluc, P., and Flucher, B. E. (2008) Auxiliary Ca^{2+} channel subunits: lessons learned from muscle. *Curr. Opin. Pharmacol.* **8,** 311–318
2. Coronado, R., Ahern, C. A., Sheridan, D. C., Cheng, W., Carbonneau, L., and Bhattacharya, D. (2004) Functional equivalence of dihydropyridine receptor α_{1S} and β_{1a} subunits in triggering excitation-contraction coupling in skeletal muscle. *Biol. Res.* **37,** 565–575
3. Wu, J., Yan, Z., Li, Z., Yan, C., Lu, S., Dong, M., and Yan, N. (2015) Structure of the voltage-gated calcium channel Cav1.1 complex. *Science* **350,** aad2395
4. Wu, J., Yan, Z., Li, Z., Qian, X., Lu, S., Dong, M., Zhou, Q., and Yan, N. (2016) Structure of the voltage-gated calcium channel Cav1.1 at 3.6 A resolution. *Nature* **537,** 191–196
5. Chen, Y. H., Li, M. H., Zhang, Y., He, L. L., Yamada, Y., Fitzmaurice, A., Shen, Y., Zhang, H., Tong, L., and Yang, J. (2004) Structural basis of the α_1-β subunit interaction of voltage-gated Ca^{2+} channels. *Nature* **429,** 675–680
6. Opatowsky, Y., Chen, C. C., Campbell, K. P., and Hirsch, J. A. (2004) Structural analysis of the voltage-dependent calcium channel β subunit functional core and its complex with the α_1 interaction domain. *Neuron* **42,** 387–399
7. Van Petegem, F., Clark, K. A., Chatelain, F. C., and Minor, D. L., Jr. (2004) Structure of a complex between a voltage-gated calcium channel β-subunit and an α-subunit domain. *Nature* **429,** 671–675
8. Richards, M. W., Butcher, A. J., and Dolphin, A. C. (2004) Ca^{2+} channel β-subunits: structural insights AID our understanding. *Trends Pharmacol. Sci.* **25,** 626–632
9. Campiglio, M., Di Biase, V., Tuluc, P., and Flucher, B. E. (2013) Stable incorporation versus dynamic exchange of β subunits in a native Ca^{2+} channel complex. *J. Cell Sci.* **126,** 2092–2101
10. Karunasekara, Y., Rebbeck, R. T., Weaver, L. M., Board, P. G., Dulhunty, A. F., and Casarotto, M. G. (2012) An α-helical C-terminal tail segment of the skeletal L-type Ca^{2+} channel β_{1a} subunit activates ryanodine receptor type 1 via a hydrophobic surface. *FASEB J.* **26,** 5049–5059
11. Eltit, J. M., Franzini-Armstrong, C., and Perez, C. F. (2014) Amino acid residues 489–503 of dihydropyridine receptor (DHPR) β_{1a} subunit are critical for structural communication between the skeletal muscle DHPR complex and type 1 ryanodine receptor. *J. Biol. Chem.* **289,** 36116–36124
12. Dayal, A., Bhat, V., Franzini-Armstrong, C., and Grabner, M. (2013) Domain cooperativity in the β_{1a} subunit is essential for dihydropyridine receptor voltage sensing in skeletal muscle. *Proc. Natl. Acad. Sci. U.S.A.* **110,** 7488–7493
13. Lao, Q. Z., Kobrinsky, E., Liu, Z., and Soldatov, N. M. (2010) Oligomerization of $Ca_v\beta$ subunits is an essential correlate of Ca2+ channel activity. *FASEB J.* **24,** 5013–5023
14. Dolphin, A. C. (2003) β subunits of voltage-gated calcium channels. *J. Bioenerg. Biomembr.* **35,** 599–620
15. McCoy, A. J., Grosse-Kunstleve, R. W., Adams, P. D., Winn, M. D., Storoni, L. C., and Read, R. J. (2007) Phaser crystallographic software. *J. Appl. Crystallogr.* **40,** 658–674
16. Ristic, M., Rosa, N., Seabrook, S. A., and Newman, J. (2015) Formulation screening by differential scanning fluorimetry: how often does it work? *Acta Crystallogr. F Struct. Biol. Commun.* **71,** 1359–1364
17. Schredelseker, J., Dayal, A., Schwerte, T., Franzini-Armstrong, C., and Grabner, M. (2009) Proper restoration of excitation-contraction coupling in the dihydropyridine receptor β_1-null zebrafish relaxed is an exclusive function of the β_{1a} subunit. *J. Biol. Chem.* **284,** 1242–1251
18. McGee, A. W., Dakoji, S. R., Olsen, O., Bredt, D. S., Lim, W. A., and Prehoda, K. E. (2001) Structure of the SH3-guanylate kinase module from PSD-95 suggests a mechanism for regulated assembly of MAGUK scaffolding proteins. *Mol. Cell* **8,** 1291–1301

ASBMB

19. Richards, M. W., Leroy, J., Pratt, W. S., and Dolphin, A. C. (2007) The HOOK-domain between the SH3 and the GK domains of $Ca_v\beta$ subunits contains key determinants controlling calcium channel inactivation. *Channels* **1,** 92–101
20. De Waard, M., Scott, V. E., Pragnell, M., and Campbell, K. P. (1996) Identification of critical amino acids involved in α_1-β interaction in voltage-dependent Ca^{2+} channels. *FEBS Lett.* **380,** 272–276
21. Hidalgo, P., Gonzalez-Gutierrez, G., Garcia-Olivares, J., and Neely, A. (2006) The α_1-β-subunit interaction that modulates calcium channel activity is reversible and requires a competent α-interaction domain. *J. Biol. Chem.* **281,** 24104–24110
22. Zhang, Y., Yamada, Y., Fan, M., Bangaru, S. D., Lin, B., and Yang, J. (2010) The β subunit of voltage-gated Ca^{2+} channels interacts with and regulates the activity of a novel isoform of Pax6. *J. Biol. Chem.* **285,** 2527–2536
23. Miranda-Laferte, E., Gonzalez-Gutierrez, G., Schmidt, S., Zeug, A., Ponimaskin, E. G., Neely, A., and Hidalgo, P. (2011) Homodimerization of the Srchomology3domainofthecalciumchannelβ-subunitdrivesdynamin-dependent endocytosis. *J. Biol. Chem.* **286,** 22203–22210
24. Catanzariti, A. M., Soboleva, T. A., Jans, D. A., Board, P. G., and Baker, R. T. (2004) An efficient system for high-level expression and easy purification of authentic recombinant proteins. *Protein Sci.* **13,** 1331–1339
25. Newman, J., Egan, D., Walter, T. S., Meged, R., Berry, I., Ben Jelloul, M., Sussman, J. L., Stuart, D. I., and Perrakis, A. (2005) Towards rationalization of crystallization screening for small- to medium-sized academic laboratories: the PACT/JCSG+ strategy. *Acta Crystallogr. D Biol. Crystallogr.* **61,** 1426–1431
26. Otwinowski, Z., and Minor, W. (1997) *Macromolecular Crystallography*, part A, Academic Press, New York
27. Emsley, P., Lohkamp, B., Scott, W. G., and Cowtan, K. (2010) Features and development of Coot. *Acta Crystallogr. D Biol. Crystallogr.* **66,** 486–501
28. Skubák, P., Murshudov, G. N., and Pannu, N. S. (2004) Direct incorporation of experimental phase information in model refinement. *Acta Crystallogr. D Biol. Crystallogr.* **60,** 2196–2201
29. Edelhoch, H. (1967) Spectroscopic determination of tryptophan and tyrosine in proteins. *Biochemistry* **6,** 1948–1954
30. Bonita, R., Beaglehole, R., and Kjellstrom, T. (2006) *Basic Epidemiology*, 2nd Ed., pp. 73–74, World Health Organization, Geneva, Switzerland